Identification and Rescue of α-Synuclein Toxicity in Parkinson Patient–Derived Neurons

Chee Yeun Chung *et al.*

Science **342**, 983 (2013);
DOI: 10.1126/science.1245296

Science (print ISSN 0036-8075; online ISSN 1095-9203) is published weekly, except the last week in December, by the American Association for the Advancement of Science, 1200 New York Avenue NW, Washington, DC 20005.

GFP from the Golgi and the vacuole (Fig. 4B). Further, in the presence of α-syn, NAB2 restored trafficking of both substrates (Fig. 4, A and B).

In addition to specific substrates, bulk endosomal transport from the plasma membrane to the vacuole was perturbed by α-syn (Fig. 4C) (*7*–*9*, *19*). When FM4-64 was used to pulse-label the endosomal pathway, after prolonged α-syn expression the dye strongly colocalized with α-syn inclusions and failed to reach the vacuole (Fig. 4C). NAB2 fully restored endocytosis and concomitantly reduced α-syn inclusions (Fig. 4C, bottom). Thus, the ability of NAB to promote Rsp5-dependent processes directly restored diverse cellular pathologies caused by α-syn, including both ER-to-Golgi and endosomal trafficking (Fig. 4D and fig. S8).

Rsp5/Nedd4 can ubiquitinate α-syn, and Nedd4 localizes to Lewy Bodies in brain samples from PD patients (*20*). However, α-syn levels were not altered by NAB2 in vivo (Fig. 1E). And when tested in vitro, NAB2 did not affect the ubiquitination of α-syn and Sna3 by Rsp5 (fig. S13). As noted, however, most of the complexities of Rsp5 in vivo activities have yet to be recapitulated in vitro. Thus, NAB2 exemplifies the ability of unbiased in vivo phenotypic screens to uncover chemical probes that cannot be discovered through simple target-based in vitro approaches. Likewise, NAB2 chemical genetics identify a deeply rooted biological node, Rsp5, that had not been identified in previous overexpression or deletion screens. Despite their central role in protein homeostasis and several human diseases, to date E3 ubiquitin ligases are virtually untouched by biological probes, let alone therapeutics.

The vesicular trafficking processes perturbed by α-syn and promoted by NAB are fundamental to all eukaryotic cells yet are particularly important to neurons that rely heavily on efficient synaptic vesicle dynamics and regulated neurotransmitter release. Indeed, dysfunctional endosomal transport is emerging as a contributing factor in α-syn pathology in human neurons. Altered cell biology, post mortem pathology, and human genetic risk factors all implicate altered vesicular trafficking (*4*, *7*–*9*, *19*, *21*–*25*). The ability of NAB to promote endosomal trafficking through Rsp5/Nedd4 and thus "reset" vesicle trafficking homeostasis, in turn, rescued several other, seemingly disparate, α-syn phenotypes. Identifying such deeply rooted pathways that ramify to affect multiple aspects of protein-folding pathology may be critical for developing disease-modifying therapies.

References and Notes

1. D. C. Swinney, J. Anthony, *Nat. Rev. Drug Discov.* **10**, 507–519 (2011).
2. V. Khurana, S. Lindquist, *Nat. Rev. Neurosci.* **11**, 436–449 (2010).
3. D. F. Tardiff, M. L. Tucci, K. A. Caldwell, G. A. Caldwell, S. Lindquist, *J. Biol. Chem.* **287**, 4107–4120 (2012).
4. A. A. Cooper *et al.*, *Science* **313**, 324–328 (2006).
5. L. J. Su *et al.*, *Dis. Model. Mech.* **3**, 194–208 (2010).
6. C. Y. Chung *et al.*, *Science* **342**, XXX (2013).
7. T. F. Outeiro, S. Lindquist, *Science* **302**, 1772–1775 (2003).
8. A. D. Gitler *et al.*, *Proc. Natl. Acad. Sci. U.S.A.* **105**, 145–150 (2008).
9. J. H. Soper, V. Kehm, C. G. Burd, V. A. Bankaitis, V. M. Lee, *J. Mol. Neurosci.* **43**, 391–405 (2011).
10. A. B. Singleton *et al.*, *Science* **302**, 841 (2003).
11. A. M. Smith, R. Ammar, C. Nislow, G. Giaever, *Pharmacol. Ther.* **127**, 156–164 (2010).
12. A. Kumar, *Methods Mol. Biol.* **416**, 117–129 (2008).
13. D. Rotin, S. Kumar, *Nat. Rev. Mol. Cell Biol.* **10**, 398–409 (2009).
14. E. Lauwers, Z. Erpapazoglou, R. Haguenauer-Tsapis, B. André, *Trends Cell Biol.* **20**, 196–204 (2010).
15. A. Menant, R. Barbey, D. Thomas, *EMBO J.* **25**, 4436–4447 (2006).
16. C. MacDonald, D. K. Stringer, R. C. Piper, *Traffic* **13**, 586–598 (2012).
17. F. Omura, Y. Kodama, T. Ashikari, *FEMS Microbiol. Lett.* **194**, 207–214 (2001).
18. E. Yeger-Lotem *et al.*, *Nat. Genet.* **41**, 316–323 (2009).
19. V. Sancenon *et al.*, *Hum. Mol. Genet.* **21**, 2432–2449 (2012).
20. G. K. Tofaris *et al.*, *Proc. Natl. Acad. Sci. U.S.A.* **108**, 17004–17009 (2011).
21. G. Esposito, F. Ana Clara, P. Verstreken, *Dev. Neurobiol.* **72**, 134–144 (2012).
22. D. A. MacLeod *et al.*, *Neuron* **77**, 425–439 (2013).
23. C. Vilariño-Güell *et al.*, *Am. J. Hum. Genet.* **89**, 162–167 (2011).
24. A. Zimprich *et al.*, *Am. J. Hum. Genet.* **89**, 168–175 (2011).
25. P. Zabrocki *et al.*, *Biochim. Biophys. Acta* **1783**, 1767–1780 (2008).

Acknowledgments: We thank A. Kumar for providing the plasmid Tn7 library; B. Wendland and L. Hicke for the Rsp5 antibody; the WIBR Genome Technology Core for Illumina Sequencing; B. Schulman (B. Schulman and H.B.K. were funded by NIH grant 5R01GM069530) and A. Goldberg for help with in vitro ubiquitination assays; T. DiCesare for graphics support; and members of the Lindquist Lab for helpful comments on the manuscript. S.L. is an investigator for HHMI. D.F.T. was funded by a National Research Service Award (NRSA) fellowship F32NS061419 and research supported by the JPB Foundation (D.F.T. and S.L.), the Eleanor Schwartz Charitable Foundation, and an HHMI Collaborative Innovation Award (D.F.T., V.K., C.Y.C., and S.L.; G.A.C., K.A.C., and M.L.T.; and J.-C.R. and M.A.T.). N.T.J. was funded by a NRSA fellowship (F32GM099817), and N.T.J. and S.L.B. were funded by NIH grant GM58160. H.T.K. was funded by the Bachmann-Strauss Dystonia & Parkinson Foundation. Genome sequencing data are deposited in the National Center for Biotechnology Information under BioProject accession number PRJNA222476. WIBR and MIT have filed a patent application, on which D.F.T., N.T.J., S.L.B., and S.L. are inventors, relating to use of compounds described here in treatment of neurodegenerative diseases. In addition, S.L. is an inventor on patents and patent applications filed by the University of Chicago relating to methods of screening for compounds that decrease α-syn–associated toxicity using yeast that express α-syn. All the yeast plasmids and strains and NAB are available under a Uniform Biological Material Transfer Agreement from the Whitehead Institute.

Supplementary Materials

www.sciencemag.org/content/342/6161/979/suppl/DC1
Materials and Methods
Supplementary Text
Figs. S1 to S13
Tables S1 to S3
References (*26*–*50*)

29 August 2013; accepted 16 October 2013
Published online 24 October 2013;
10.1126/science.1245321

Identification and Rescue of α-Synuclein Toxicity in Parkinson Patient–Derived Neurons

Chee Yeun Chung,[1]* Vikram Khurana,[1,2]* Pavan K. Auluck,[1,3] Daniel F. Tardiff,[1] Joseph R. Mazzulli,[2] Frank Soldner,[1] Valeriya Baru,[1,4] Yali Lou,[1,4] Yelena Freyzon,[1] Sukhee Cho,[5] Alison E. Mungenast,[5] Julien Muffat,[1] Maisam Mitalipova,[1] Michael D. Pluth,[6] Nathan T. Jui,[6] Birgitt Schüle,[7] Stephen J. Lippard,[6] Li-Huei Tsai,[4,5] Dimitri Krainc,[2] Stephen L. Buchwald,[6] Rudolf Jaenisch,[1,8] Susan Lindquist[1,4,8]†

The induced pluripotent stem (iPS) cell field holds promise for in vitro disease modeling. However, identifying innate cellular pathologies, particularly for age-related neurodegenerative diseases, has been challenging. Here, we exploited mutation correction of iPS cells and conserved proteotoxic mechanisms from yeast to humans to discover and reverse phenotypic responses to α-synuclein (αsyn), a key protein involved in Parkinson's disease (PD). We generated cortical neurons from iPS cells of patients harboring αsyn mutations, who are at high risk of developing PD dementia. Genetic modifiers from unbiased screens in a yeast model of αsyn toxicity led to identification of early pathogenic phenotypes in patient neurons. These included nitrosative stress, accumulation of endoplasmic reticulum (ER)–associated degradation substrates, and ER stress. A small molecule identified in a yeast screen (NAB2), and the ubiquitin ligase Nedd4 it affects, reversed pathologic phenotypes in these neurons.

Neurodegenerative dementias are devastating and incurable diseases for which we need tractable cellular models to investigate pathologies and discover therapeutics. Parkinson's disease dementia (PDD), a debilitating nonmotor manifestation of Parkinson's disease (PD), affects as many as 80% of patients (*1*). The best pathological correlate of PDD is neuron loss and pathological aggregation of α-synuclein (αsyn) within deep layers of the cerebral cortex (*1*). Contursi kindred patients, who harbor an autosomal dominant and highly penetrant $Ala^{53}\rightarrow Thr^{53}$ (A53T) mutation in αsyn, manifest prominent PD and dementia (*2*, *3*). Induced pluripotent stem (iPS) cells from a female member of this kindred (table S1) have recently been mutation-corrected to control for genetic background effects (*4*). To establish a model for cortical synucleinopathy, we differentiated

two pairs of subclones from these lines (fig. S1) into cortical neurons (see supplementary materials and methods and figs. S2 and S3).

Over 12 weeks of differentiation, cultures consisted primarily of excitatory glutamatergic neurons mixed with glia (figs. S2, C to E, and S3). To identify neurons, we infected neural precursors before differentiation with lentiviruses expressing enhanced yellow fluorescent protein or red fluorescent protein (RFP) under the control of the synapsin promoter (fig. S2G). When cocultured, A53T and corrected neurons were electrically active at 8 weeks of differentiation. They exhibited similar calcium fluxes and electrophysiology (fig. S2, H and I). The majority of neurons were immunopositive for Tbr1, a transcription factor indicating developing deep cortical layers (fig. S2E) (*5*). αsyn was robustly expressed, but only after neuronal differentiation (fig. S2, C to F). In neuronal processes, αsyn was both cytoplasmic and punctate (fig. S2, C to E). Thus, these cells provide a relevant substrate for examining early αsyn-related cortical pathologies.

It has been difficult to establish neurodegenerative phenotypes in iPS cell–derived neurons that can be solely attributable to disease-causing genetic mutations. Previous studies accelerated degenerative phenotypes with toxins such as oxidative stressors (*6*–*8*). In addition, inconsistent differentiation precludes these cells from being used in high-throughput screening. To address these problems, we turned to a yeast platform in which αsyn-expression results in toxicity (*9*, *10*) and disease-relevant phenotypes, including focal accumulation of αsyn, mitochondrial dysfunction, αsyn-mediated vesicle trafficking defects, links to genetic and environmental risk factors, and sensitivity to αsyn dosage (*9*–*12*). We reasoned that unbiased genetic analysis in this system could guide discovery of innate pathological phenotypes.

Previous unbiased yeast genetic screens, encompassing 85% of the yeast proteome, identified robust modifiers of αsyn toxicity (*9*, *12*). We first tested Fzf1, a transcriptional regulator of nitrosative stress responses (*13*) that suppressed αsyn toxicity in yeast (Fig. 1A). Nitrosative stress is caused by nitric oxide (NO) and related redox forms. Though it is not known if there is a direct causal connection between nitrosative stress and αsyn toxicity, the nitration of tyrosine residues is increased in postmortem brain samples from synucleinopathy patients (*14*, *15*).

To determine if nitrative damage occurs to yeast proteins in direct response to αsyn, we took advantage of an antibody to nitrotyrosine. In yeast, this antibody exhibited minimal background in control strains, allowing us to detect intense protein nitration that was tightly dependent on αsyn dosage (Fig. 1B). Nitration was a highly specific response to αsyn toxicity and was not observed with other neurodegenerative disease proteins expressed at equally toxic levels, including amyloid β peptide, TDP-43, polyQ-expanded Huntingtin, and Fus (Fig. 1B).

Expression of Fzf1 strongly decreased protein nitration induced by αsyn (Fig. 1C). Next, we asked if αsyn toxicity could be tuned by altering the production of NO. In yeast, NO levels are regulated by switching between distinct isoforms of mitochondrial cytochrome c oxidase (COX5): Deletion of COX5A increases NO; deletion of COX5B decreases it (*16*). Indeed, these manipulations increased and decreased nitrotyrosine levels in response to αsyn (Fig. 1D). Toxicity increased and decreased commensurately (Fig. 1E). Thus, in yeast, nitrosative stress is not simply a consequence of αsyn toxicity but also contributes to toxicity.

To investigate a connection between αsyn and nitrosative stress in neurons, we employed FL2, a copper and fluorescein–based NO sensor (*17*). We optimized the use of FL2 with rat primary cortical cultures (fig. S4), a neuronal synucleinopathy model. Overexpression of αsyn increased the FL2 signal, with a perinuclear distribution in the cell body (Fig. 2A, top) that partially colocalized with the endoplasmic reticulum (ER) (Fig. 2A, bottom). High density of processes and mixed cell types hindered intensity measurements outside of well-defined neuronal cell bodies.

Having optimized the FL2 assay in rat neurons, we turned to our Parkinson patient–derived cortical neurons at 8 weeks of differentiation. Two isogenic pairs of A53T and mutation-corrected neurons were differentiated in parallel and labeled with synapsin-RFP (fig. S2G). Intraneuronal FL2 signals increased in A53T neurons relative to corrected neurons, again most readily visualized in the cell body (Fig. 2B, top). As in rodent neurons, we observed partial colocalization of this signal with an ER marker (Fig. 2B, bottom). Cytoplasmic nitrotyrosine staining also accumulated in mutant neurons compared with corrected neurons (Fig. 2C). Similarly, cytoplasmic nitrotyrosine staining was prominent in neurons and neuropil of the postmortem frontal cortex from another patient

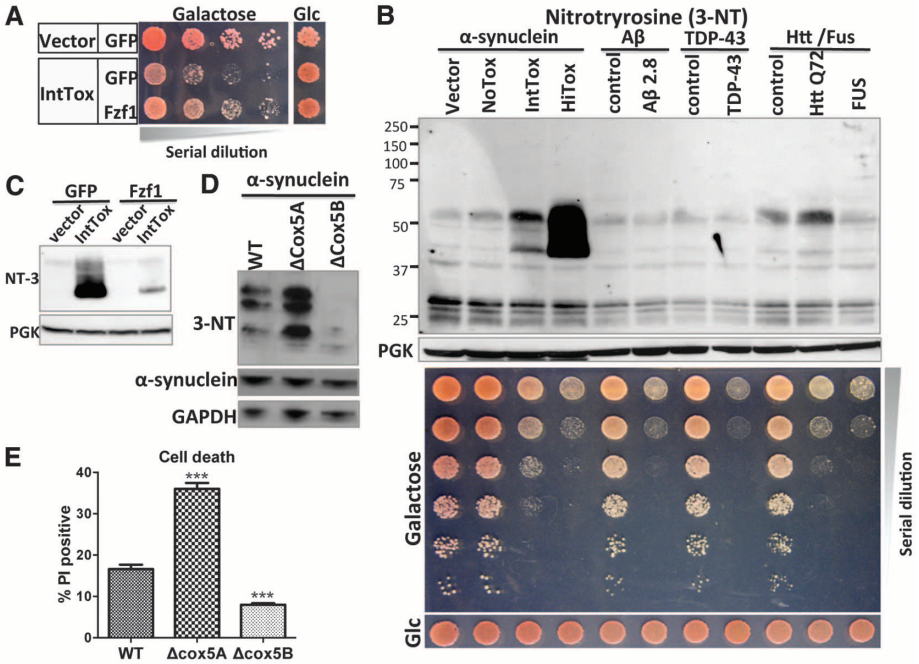

Fig. 1. A specific link between αsyn toxicity and nitrosative stress is identified in yeast. (**A**) Fzf1 overexpression reduces αsyn toxicity in yeast (IntTox), measured by growth of serially diluted yeast. GFP, green fluorescent protein; Glc, glucose. (**B**) Protein nitration levels were measured by immunoblotting for 3-nitrotyrosine (3-NT). Strains expressing low (NoTox), intermediate (IntTox), and high (HiTox) levels of αsyn were analyzed (*11*). Neurodegeneration-related models with equivalent toxicity [expressing Aβ (β-amyloid peptide), Htt72Q (Huntingtin exon 1 with 72 glutamines), or Fus] were not similarly affected. PGK, phosphoglycerate kinase. (**C**) Fzf1 expression reduced αsyn-induced increase in nitration. (**D** and **E**) NO-increasing deletion of Cox5A (ΔCox5A) increased protein nitration levels, whereas the NO-decreasing Cox5B deletion (ΔCox5B) reduced protein nitration levels (D). Toxicity was determined by flow cytometry with propidium iodide (PI)–stained cells (E). Data are represented as mean ± SEM (error bars). ***$P < 0.001$ [one-way analysis of variance (ANOVA) with Bonferroni post hoc test]. WT, wild type.

[1]Whitehead Institute for Biomedical Research, Cambridge, MA 02142, USA. [2]Department of Neurology, Massachusetts General Hospital and Harvard Medical School, Boston, MA 02114, USA. [3]Department of Pathology (Neuropathology), Massachusetts General Hospital and Harvard Medical School, Boston, MA 02114, USA. [4]Howard Hughes Medical Institute, Department of Biology, Massachusetts Institute of Technology, Cambridge, MA, USA. [5]The Picower Institute for Learning and Memory, Department of Brain and Cognitive Sciences, Massachusetts Institute of Technology, Cambridge, MA 02139, USA. [6]Department of Chemistry, Massachusetts Institute of Technology, Cambridge, MA 02139, USA. [7]The Parkinson's Institute, Sunnyvale, CA 94085,USA. [8]Department of Biology, Massachusetts Institute of Technology, Cambridge, MA, USA.

*These authors contributed equally to this work.
†Corresponding author. E-mail: lindquist_admin@wi.mit.edu

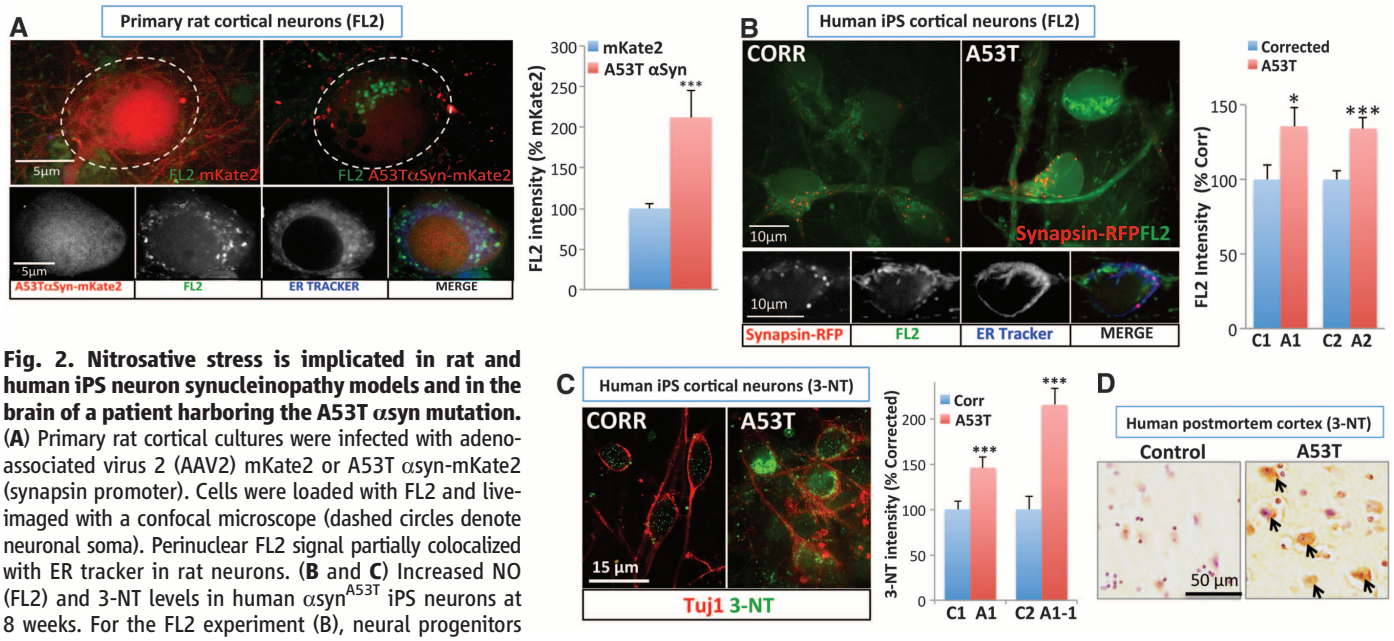

Fig. 2. Nitrosative stress is implicated in rat and human iPS neuron synucleinopathy models and in the brain of a patient harboring the A53T αsyn mutation. (**A**) Primary rat cortical cultures were infected with adeno-associated virus 2 (AAV2) mKate2 or A53T αsyn-mKate2 (synapsin promoter). Cells were loaded with FL2 and live-imaged with a confocal microscope (dashed circles denote neuronal soma). Perinuclear FL2 signal partially colocalized with ER tracker in rat neurons. (**B** and **C**) Increased NO (FL2) and 3-NT levels in human αsyn^{A53T} iPS neurons at 8 weeks. For the FL2 experiment (B), neural progenitors were transduced with lentivirus-RFP (synapsin promoter) to mark neurons. CORR, mutation-corrected neurons. (**D**) Postmortem frontal cortex from a patient harboring A53T mutation exhibited increased 3-NT immunoreactivity. Arrows indicate cells immunopositive for 3-NT. All data are represented as mean ± SEM. $^{*}P < 0.05$; $^{***}P < 0.001$ (two-tail t test).

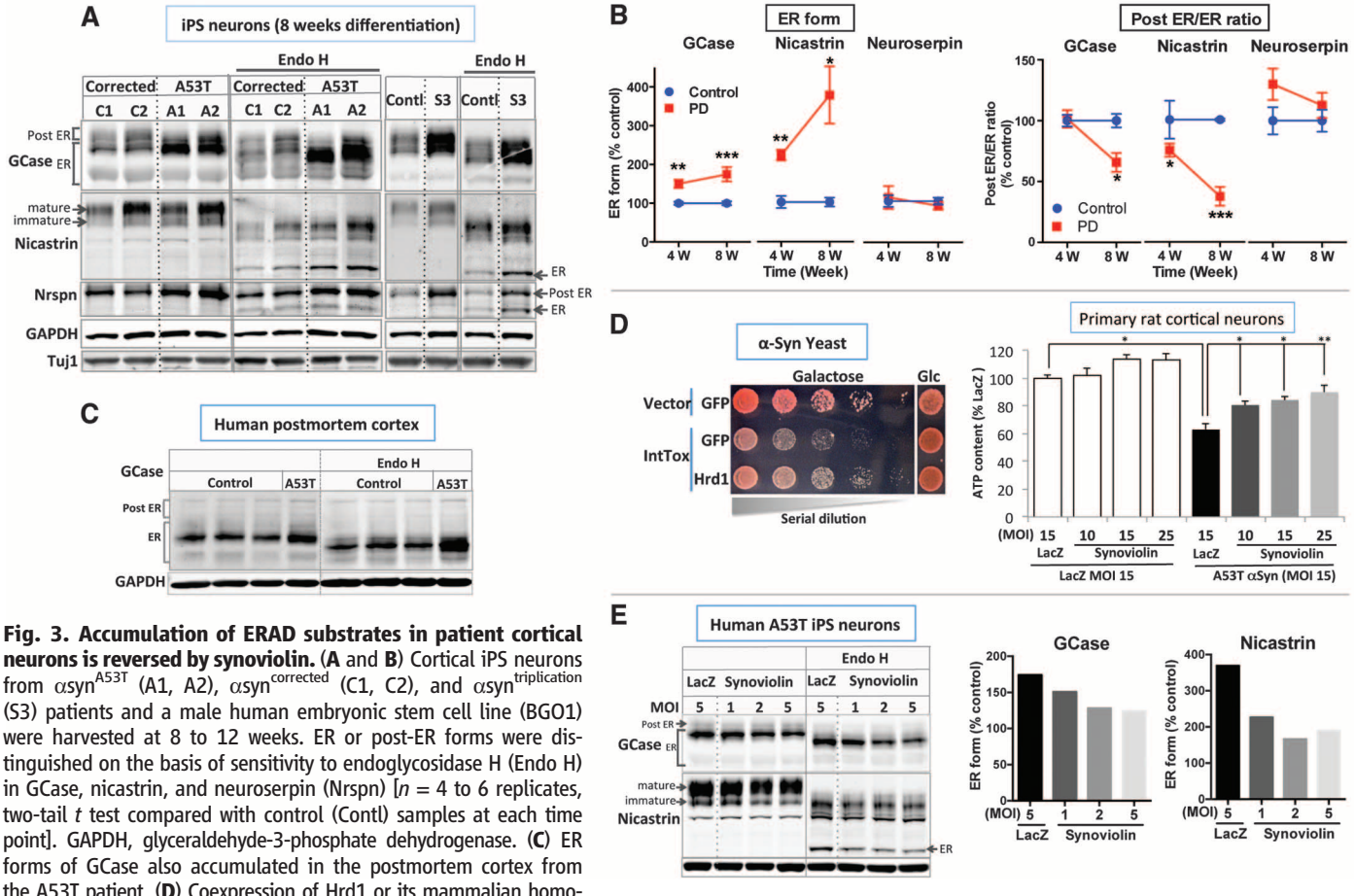

Fig. 3. Accumulation of ERAD substrates in patient cortical neurons is reversed by synoviolin. (**A** and **B**) Cortical iPS neurons from αsyn^{A53T} (A1, A2), $\alpha syn^{corrected}$ (C1, C2), and $\alpha syn^{triplication}$ (S3) patients and a male human embryonic stem cell line (BGO1) were harvested at 8 to 12 weeks. ER or post-ER forms were distinguished on the basis of sensitivity to endoglycosidase H (Endo H) in GCase, nicastrin, and neuroserpin (Nrspn) [$n = 4$ to 6 replicates, two-tail t test compared with control (Contl) samples at each time point]. GAPDH, glyceraldehyde-3-phosphate dehydrogenase. (**C**) ER forms of GCase also accumulated in the postmortem cortex from the A53T patient. (**D**) Coexpression of Hrd1 or its mammalian homolog, synoviolin, reduced αsyn toxicity in yeast and rat cortical neurons. Rat cultures were transduced by lentivirus encoding synoviolin with varying multiplicity of infection (MOI) and cotransduced with lenti-αsyn^{A53T} or lenti-LacZ. Cellular adenosine triphosphate (ATP) content was measured (one-way ANOVA with Bonferroni post hoc test). (**E**) Lentiviral transduction of synoviolin reduced accumulation of ER forms of GCase and nicastrin in αsyn^{A53T} iPS cortical neurons at 8 to 12 weeks. Baseline PD levels were equated to the percentage of control established in Fig. 3 to depict biological importance of the change. All data are represented as mean ± SEM. $^{*}P < 0.05$; $^{**}P < 0.01$; $^{***}P < 0.001$.

in the same kindred (*18*), but not in control brain samples (Fig. 2D).

The yeast synucleinopathy model exhibits ER stress, ER-associated degradation (ERAD) substrate accumulation, and defective trafficking from the ER to Golgi (*12*). ER stress has also been described in a mouse synucleinopathy model (*19*). Because NO was visualized in the vicinity of the ER in neurons (Fig. 2), we asked whether modulating NO levels modulates ER stress. Indeed, manipulating COX5 isoforms to increase and decrease NO levels commensurately altered the unfolded protein response (fig. S5A) and the ER accumulation of carboxypeptidase Y (CPY) (fig. S5B), a well-characterized ERAD substrate that traffics between the ER and vacuole (*12*). This required the presence of αsyn (fig. S5A), implying a connection between nitrosative and ER stress in the context of αsyn toxicity. Correspondingly, two hallmarks of ER stress—protein disulfide isomerase and binding immunoglobulin protein—increased at 12 weeks of differentiation in the A53T neurons compared with corrected cells (fig. S5C). Levels of CHOP (CCAAT enhancer-binding protein homologous protein), a component of ER stress-induced apoptosis, did not change (fig. S5C), indicating that cellular pathology was still at an early stage.

Next, we assessed the accumulation and trafficking of three ERAD substrates implicated in neurodegeneration: glucocerebrosidase (GCase), neuroserpin, and nicastrin (*20*). GCase mutations are common risk factors for PD and confer risk for cognitive impairment in this disease (*21*). GCase accumulates in the ER of cultured cells overexpressing αsyn (*22*). ER forms of GCase and nicastrin accumulated, and the ratio of post-ER–to–ER forms declined in A53T compared with mutation-corrected patient neurons starting at 4 weeks (Fig. 3, A and B, and fig. S6, A to C). Neuroserpin was not affected at the time points we examined (Fig. 3, A and B, and fig. S6, A to C). Levels of neuron-specific markers were unaffected (Fig. 3A and fig. S6C). These findings were consistent in multiple rounds of differentiation and robust-to-distinct differentiation protocols (fig. S6C). Phenotypes were not present in the undifferentiated iPS cell lines (fig. S6D). Thus, ERAD dysfunction is an early and progressive cellular phenotype in response to mutated αsyn in patient neurons.

The increase in the ER form of GCase and the decrease in the post-ER–to–ER ratio were recapitulated in the brain of an A53T patient (Fig. 3C and fig. S7B). Cortices from sporadic PD samples exhibited the same trend (fig. S7). We also analyzed cortical neurons generated from the iPS cells of a male patient of the Iowa kindred. This patient harbored a triplication of the wild-type αsyn gene and manifested aggressive dementia, in addition to parkinsonism (table S1). Aged cortical neurons generated from the male human embryonic stem cell line BG01 (*23*) served as a control. ERAD substrates accumulated (Fig. 3A and fig. S6B) and ER stress increased (fig. S5C) in neurons from this patient, closely phenocopying A53T cells.

Another suppressor of αsyn toxicity recovered in the yeast screen was Hrd1 (Fig. 3D, left) (*9*). Hrd1 is a highly conserved E3 ubiquitin ligase (synoviolin-1 or Syvn1 in humans) that plays a critical role in ERAD from yeast to human. In primary rat cortical neurons, lentiviral expression of Syvn1 rescued αsyn toxicity in a dose-dependent manner (Fig. 3D, right). Syvn1 also reduced nicastrin and GCase accumulation in the ER of the A53T patient cortical neurons (Fig. 3E).

Next, we tested the ability of NAB2 (*24*) to rescue the pathological phenotypes we discovered here in both yeast cells and PD neurons. NAB2, an *N*-arylbenzimidazole, was recovered in a yeast screen of more than 180,000 small molecules and rescues αsyn toxicity in yeast by activating the Rsp5-Nedd4 pathway (*24*). This protein is another highly conserved ubiquitin ligase and plays a key role in regulating vesicle trafficking (*25*, *26*). NAB2 reduced protein nitration in the yeast synucleinopathy model (Fig. 4A) and decreased NO levels in A53T patient neurons (Fig. 4B). Moreover, NAB2 reduced the accumulation of immature ER forms of CPY in yeast (Fig. 4A). This molecule increased the post-ER forms and decreased the immature forms of nicastrin and GCase in PD patient neurons (Fig. 4C and fig. S8). Furthermore, NAB2 analogs that were inactive in yeast (*24*) were also inactive in human neurons (fig. S9). Connecting NAB2 back to the ubiquitin ligase, we used a lentivirus to overexpress Nedd4. This phenocopied the effects of the compound, increasing the mature forms of nicastrin and GCase (Fig. 4D).

Conserved biology in a cross-species cellular discovery platform, as described here, enabled the

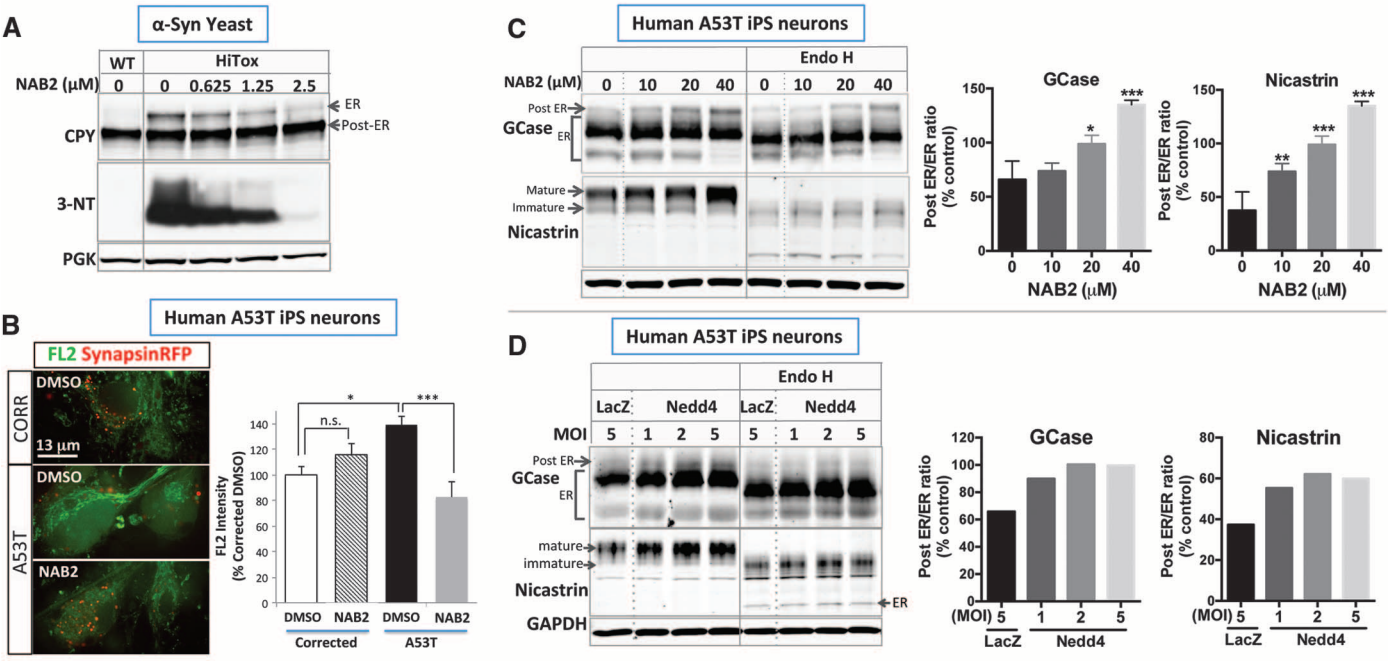

Fig. 4. A small-molecule modifier, identified in an unbiased yeast screen, and its target correct analogous defects in yeast and patient neurons. (**A**) NAB2 ameliorates αsyn-induced ER accumulation of CPY and nitrosative stress in the yeast model. (**B**) NAB2 (5 μM) decreases nitric oxide (FL2) levels in αsyn^{A53T} iPS neurons labeled with synapsin-RFP. DMSO, dimethyl sulfoxide. (**C**) NAB2 increases post-ER forms of and ameliorates the ER accumulation of GCase and nicastrin in αsyn^{A53T} iPS neurons. (**D**) Lentiviral delivery of Nedd4 phenocopies the NAB2 treatment, increasing mature forms of GCase and nicastrin. Baseline PD levels were equated to the percentage of control established in Fig. 3. All data are represented as mean ± SEM; n.s., not significant. *$P < 0.05$; **$P < 0.01$; ***$P < 0.001$ (two-tail *t* test compared with control condition).

discovery of innate pathologic phenotypes in neurons derived from patients with PD. It also enabled the identification of genes and small molecules that reverted these phenotypes (*24*) (fig. S10). A similar approach might be useful in the study of other PD-relevant phenotypes identified in yeast, including mitochondrial dysfunction and perturbed metal-ion homeostasis (*9*, *11*). The existence of other yeast models of neurodegenerative diseases suggests that this approach may also be generalizable to other diseases (*11*, *27*, *28*).

References and Notes

1. D. J. Irwin *et al.*, *Ann. Neurol.* **72**, 587–598 (2012).
2. P. J. Spira, D. M. Sharpe, G. Halliday, J. Cavanagh, G. A. Nicholson, *Ann. Neurol.* **49**, 313–319 (2001).
3. K. Markopoulou *et al.*, *Acta Neuropathol.* **116**, 25–35 (2008).
4. F. Soldner *et al.*, *Cell* **146**, 318–331 (2011).
5. T. Saito *et al.*, *Cereb. Cortex* **21**, 588–596 (2011).
6. H. N. Nguyen *et al.*, *Cell Stem Cell* **8**, 267–280 (2011).
7. B. Byers *et al.*, *PLOS ONE* **6**, e26159 (2011).
8. O. Cooper *et al.*, *Sci. Transl. Med.* **4**, 141ra90 (2012).
9. A. D. Gitler *et al.*, *Nat. Genet.* **41**, 308–315 (2009).
10. T. F. Outeiro, S. Lindquist, *Science* **302**, 1772–1775 (2003).
11. V. Khurana, S. Lindquist, *Nat. Rev. Neurosci.* **11**, 436–449 (2010).
12. A. A. Cooper *et al.*, *Science* **313**, 324–328 (2006).
13. A. Sarver, J. DeRisi, *Mol. Biol. Cell* **16**, 4781–4791 (2005).
14. B. I. Giasson *et al.*, *Science* **290**, 985–989 (2000).
15. E. Gómez-Tortosa *et al.*, *Acta Neuropathol.* **103**, 495–500 (2002).
16. P. R. Castello *et al.*, *Proc. Natl. Acad. Sci. U.S.A.* **105**, 8203–8208 (2008).
17. M. D. Pluth, E. Tomat, S. J. Lippard, *Annu. Rev. Biochem.* **80**, 333–355 (2011).
18. P. T. Kotzbauer *et al.*, *Exp. Neurol.* **187**, 279–288 (2004).
19. E. Colla *et al.*, *J. Neurosci.* **32**, 3306–3320 (2012).
20. K. Tabuchi, G. Chen, T. C. Südhof, J. Shen, *J. Neurosci.* **29**, 7290–7301 (2009).
21. R. N. Alcalay *et al.*, *Neurology* **78**, 1434–1440 (2012).
22. J. R. Mazzulli *et al.*, *Cell* **146**, 37–52 (2011).
23. M. Mitalipova *et al.*, *Stem Cells* **21**, 521–526 (2003).
24. D. F. Tardiff *et al.*, *Science* **342**, 979–983 (2013).
25. C. M. Haynes, S. Caldwell, A. A. Cooper, *J. Cell Biol.* **158**, 91–102 (2002).
26. P. Donovan, P. Poronnik, *Int. J. Biochem. Cell Biol.* **45**, 706–710 (2013).
27. A. C. Elden *et al.*, *Nature* **466**, 1069–1075 (2010).
28. S. Treusch *et al.*, *Science* **334**, 1241–1245 (2011).

Acknowledgments: We thank D. Dickson, L. Golbe, and J. Trojanowki for postmorterm tissue or data; D. Pincus for the UPR reporter; I. Cheeseman, J. Kim, J. Pruszak, P. Wisniewski, and W. Salmon for important technical advice; R. Alagappan, T. Lungiangwa, and P. Xu for superb technical assistance; and S. Santagata, L. Whitesell, M. Feany, D. Landgraf, and L. Clayton for fruitful discussion and critical comments on the manuscript. Grant support was provided by a Howard Hughes Medical Institute Collaborative Innovation Award (S.L.), JPB Foundation grants (S.L.), NIH/National Institute on Aging grant K01 AG038546 (C.Y.C.), an American Brain Foundation and Parkinson's Disease Foundation Clinician-Scientist Development Award (V.K.), NIH grant 5 R01CA084198 (R.J.), and the NSF (S.J.L.). Whitehead Institute for Biomedical Research has filed a patent application, on which authors V.K., C.Y.C., and S.L. are inventors, relating to the use of yeast- and iPS cell–based models of synucleinopathies and associated phenotypes for identifying compounds. In addition, author S.L. is an inventor on patents and patent applications filed by The University of Chicago relating to methods of screening for compounds that decrease α-synuclein–associated toxicity using yeast that expresses α-synuclein. All the yeast plasmids and strains and NAB2 are available under a Uniform Biological Material Transfer Agreement from the Whitehead Institute. Author contributions: C.Y.C., V.K., and S.L. conceptualized the study, designed the experiments, and wrote the paper. V.K. developed the human iPS cell–derived cortical synucleinopathy model, assisted by Y.L. Pluripotent cell lines, advice on experimental design, and technical expertise were provided by F.S., J.R.M., J.M., M.M., and R.J. F.S. reprogrammed the WIBR-IPS-SYN^{TRPL} line from fibroblasts provided by B.S. C.Y.C. developed the rat cortical synucleinopathy model, assisted by V.B. The mKate2-tagged constructs were generated by Y.F. C.Y.C. and V.K. performed all experiments except Fig. 1, D and E, Fig. 2E, and fig. S5, A and B (P.K.A.); Fig. 4A (D.F.T.); Fig. 4C and fig. S6C (J.R.M./D.K.); fig. S2, H and I (A.E.M./S.C./L.-H.T.); and fig. S1 (Y.F./Y.L.). The small molecule NAB2 was synthesized by N.T.J. and S.L.B., based on a yeast screen performed by D.F.T. FL2 dye synthesis and technical advice were provided by M.D.P. and S.J.L.

Supplementary Materials

www.sciencemag.org/content/342/6161/983/suppl/DC1
Materials and Methods
Figs. S1 to S10
Table S1
References (*29*–*40*)

29 August 2013; accepted 16 October 2013
Published online 24 October 2013;
10.1126/science.1245296

The Human Language–Associated Gene SRPX2 Regulates Synapse Formation and Vocalization in Mice

G. M. Sia,[1,2] R. L. Clem,[3] R. L. Huganir[1,2]*

Synapse formation in the developing brain depends on the coordinated activity of synaptogenic proteins, some of which have been implicated in a number of neurodevelopmental disorders. Here, we show that the sushi repeat–containing protein X-linked 2 (*SRPX2*) gene encodes a protein that promotes synaptogenesis in the cerebral cortex. In humans, *SRPX2* is an epilepsy- and language-associated gene that is a target of the foxhead box protein P2 (FoxP2) transcription factor. We also show that FoxP2 modulates synapse formation through regulating SRPX2 levels and that SRPX2 reduction impairs development of ultrasonic vocalization in mice. Our results suggest FoxP2 modulates the development of neural circuits through regulating synaptogenesis and that SRPX2 is a synaptogenic factor that plays a role in the pathogenesis of language disorders.

Synapse formation is an essential process during brain development that is coordinated by many membrane and secreted proteins (*1*–*5*). Proper development of neural circuitry is required for brain function, and mutations in synaptogenic genes have been linked to many cognitive diseases, including autism, schizophrenia, and mental retardation (*6*–*8*). Although a number of proteins have been shown to modulate synaptogenesis, no single gene knockout has been shown to completely ablate the formation of any major class of synapses, suggesting that the brain may use many proteins to regulate this process. To search for synaptogenic factors, we embarked on a high-throughput overexpression screen for human genes encoding membrane and secreted proteins that mediate synaptogenesis in the central nervous system. We identified sushi repeat–containing protein X-linked (SRPX2) as a secreted protein that modulates synapse density in dissociated hippocampal neurons. The *SRPX2* gene is mutated in human patients suffering from rolandic (sylvian) epilepsy with associated oral and speech dyspraxia (*9*) and is a target of the *FoxP2* gene (*10*), suggesting that SRPX2 may be involved in neural connectivity and language in humans. Although sushi domain proteins, also known as complement control protein (CCP) domain proteins, function as regulators of the immune system in vertebrates (*11*), they also regulate neuronal development in *C. elegans* (*12*) and *Drosophila* (*13*, *14*). We therefore decided to further examine the role of SRPX2 in synapse formation.

To verify that SRPX2 controls synapse density, we overexpressed rat and human *SRPX2* genes in dissociated rat cortical cells. Overexpression of SRPX2 caused an increase in the density of vesicular glutamate transporter 1 (VGlut1) and PSD-95 puncta on the neurons while leaving the density of inhibitory synaptic markers vesicular γ-aminobutyric acid (GABA) transporter (VGAT) and gephyrin unchanged (Fig. 1, A and B). Dendritic morphology was unaffected by SRPX2 overexpression (fig. S3A). Both human and rat *SRPX2* genes are capable of increasing spine density when overexpressed (Fig. 1C). Thus, SRPX2 overexpression increases the density of excitatory synapses and spines in vitro without an effect on inhibitory synapse formation.

SRPX2 mRNA is found in neurons in multiple brain regions, including the cerebral cortex and hippocampus (*9*, *15*). To further characterize the expression and localization of SRPX2 at the protein level, we generated an antibody against SRPX2 and used it to perform immunocytochemistry on

[1]Howard Hughes Medical Institute, Johns Hopkins University School of Medicine, 725 North Wolfe Street, Baltimore, MD 21205, USA. [2]Department of Neuroscience, Johns Hopkins University School of Medicine, 725 North Wolfe Street, Baltimore, MD 21205, USA. [3]Friedman Brain Institute, Mount Sinai School of Medicine, 1425 Madison Avenue, New York, NY 10029, USA.

*Corresponding author. E-mail: rhuganir@jhmi.edu